JVI Journals.ASM.org

Morphogenesis of Mimivirus and Its Viral Factories: an Atomic Force Microscopy Study of Infected Cells

Yuri G. Kuznetsov,[a] Thomas Klose,[b] Michael Rossmann,[b] Alexander McPherson[a]

Department of Molecular Biology and Biochemistry, University of California, Irvine, California, USA[a]; Department of Biological Sciences, Purdue University, West Lafayette, Indiana, USA[b]

Amoebas infected with mimivirus were disrupted at sequential stages of virus production and were visualized by atomic force microscopy. The development of virus factories proceeded over 3 to 4 h postinfection and resulted from the coalescence of 0.5- to 2-μm vesicles, possibly bearing nucleic acid, derived from either the nuclear membrane or the closely associated rough endoplasmic reticulum. Virus factories actively producing virus capsids on their surfaces were imaged, and this allowed the morphogenesis of the capsids to be delineated. The first feature to appear on a virus factory surface when a new capsid is born is the center of a stargate, which is a pentameric protein oligomer. As the arms of the stargate grow from the pentamer, a rough disk the diameter of a capsid thickens around it. This marks the initial emergence of a protein-coated membrane vesicle. The capsid self-assembles on the vesicle. Hillocks capped by different pentameric proteins spontaneously appear on the emerging vesicle at positions that are ultimately occupied by 5-fold icosahedral vertices. A lattice of coat protein nucleates at each of the 5-fold vertices, but not at the stargate, and then spreads outward from the vertices over the surface, merging seamlessly to complete the icosahedral capsid. Filling with DNA and associated proteins occurs by the transfer of nucleic acid from the interior of the virus factory into the nearly completed capsids. The portal, through which the DNA enters, is sealed by a plug of protein having a diameter of about 40 nm. A layer of integument protein that anchors the surface fibers is acquired by the passage of capsids through a membrane enriched in the protein. The coating of surface fibers is similarly acquired when the integument protein-coated capsids pass through a second membrane that has a forest of surface fibers embedded on one side.

Mimivirus (*Acanthamoeba polyphaga mimivirus*) is one of nature's largest characterized viruses, having a diameter of 700 to 750 nm based on electron microscopy (EM) (1–3) and atomic force microscopy (AFM) (4), with a genome size of 1.2 million base pairs (5), nearly twice that of any other known virus. Its linear, double-stranded DNA codes for 911 genes, and among these are many that are not expressed by any other virus but only by living cells. It is the focus of particular interest because its genomic, metabolic, and structural intricacies suggest that it might provide an evolutionary bridge between viruses and living cells (6–9). Mimivirus infects the amoeba *Acanthamoeba polyphaga*, although its host range is likely to be considerably larger (10). It appears to be most closely related structurally to large algal viruses such as *Paramecium bursaria* chlorella virus 1 (PBCV-1) and other iridoviruses (11–13), although it possesses additional features not present in those viruses.

The work of Xiao et al. (2) and Kuznetsov et al. (4) added significant detail to previous studies of the virus by Suzan-Monti et al. (14) and the group of Minsky (3), particularly regarding the structure of the icosahedral capsid and superior layers, including the surface fibers. Some of the major structural features of the virus are reviewed in the AFM images shown in Fig. 1. The capsid consists of 20 large triangular plates joined at their edges to produce twelve 5-fold vertices. The capsid surface is composed of trimeric major capsid proteins, each subunit of which consists of two jelly roll beta barrels (15) arranged in an open hexagonal lattice, which produces the impression of a honeycomb. The center-to-center distance of the capsomeres is 14 nm. Because of some remaining uncertainty in the capsid architecture, the triangulation number, T, could have any one of nine possibilities lying between 972 and 1,200 (2).

The fibers that coat particles, whose exact origins are also unknown, have nonuniform lengths of 125 nm to 140 nm and are anchored to an integument layer of protein disposed immediately above the capsid. How the integument layer is added to the capsid and how the layer of surface fibers is added atop were, until now, not known. The most striking and unique feature of mimivirus is a prominent five-armed, star-shaped apparatus that occupies a unique vertex of every virion. The star-shaped assembly, which has been termed a "stargate" (3), opens up once the virus is inside the host cell, and the DNA of the virus, enclosed in a membrane sac, emerges from the interior, fuses with a cellular membrane, and delivers its nucleic acid contents to the cell. The DNA does not enter the capsid through the stargate during virion assembly but enters through a separate portal in the center of a distal icosahedral face (3).

The work of Mutsafi et al. (16) places mimivirus in the family of large cytoplasmic viruses, and evidence was presented that the DNA of the virus never enters the host cell nucleus but that all replication occurs in the cytoplasm. This is in some disagreement with previous studies (14) that suggested otherwise. It is agreed, however, that virion synthesis occurs at "virus factories." Virus factories are distinct bodies that form in the cell cytoplasm at about 4 to 5 h postinfection (p.i.) and are responsible for, at the least, the synthesis of the icosahedral capsids and their filling by viral DNA along with associated proteins and, probably, RNA

Received 23 May 2013 **Accepted** 1 August 2013
Published ahead of print 7 August 2013
Address correspondence to Alexander McPherson, amcphers@uci.edu.

doi:10.1128/JVI.01372-13

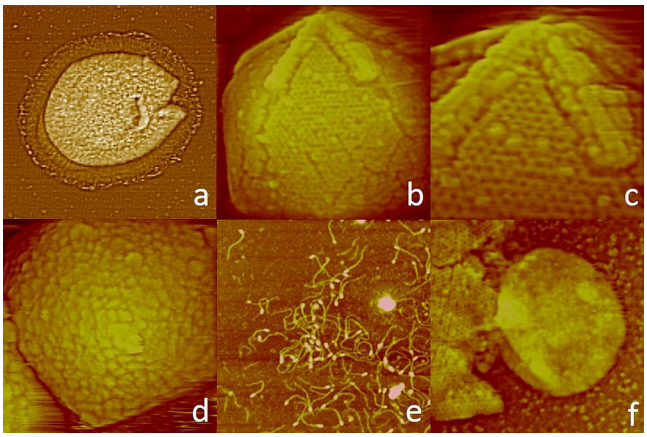

FIG 1 Mimivirus structural review. (a) Intact mimivirus about 750 nm in diameter with a characteristic corona of surface fibers. Its stargate is just beginning to open at the right. (b) Icosahedral capsid of mimivirus, which has been exposed by treatment of the virus with lysozyme and bromelain to remove superior layers. The stargate is at the top. (c) Higher-magnification image of the stargate showing some details of its multilayer construction. The arms of the stargate split along their lengths and then fall away as the stargate opens. The icosahedral protein lattice making up the capsid is apparent. (d and e) Capsid coated in turn with a layer of membrane-associated integument protein (d) that is responsible for anchoring the surface fibers (e). With integument protein added, but without surface fibers, the capsid is about 450 nm in diameter. The surface fibers are 125 to 140 nm in length and are tipped with a globular protein head. (f) AFM image capturing the opening of the stargate of a capsid to release the internal membrane sac, derived from a membrane near the surface of a viral factory, containing the genomic DNA and its associated proteins. Scan areas are 1.5 μm by 1.5 μm (a), 500 nm by 500 nm (b), 250 nm by 250 nm (c), 500 nm by 500 nm (d), 1 μm by 1 μm (e), and 625 nm by 625 nm (f).

(17). There is little information regarding the morphogenesis of the capsid within the virus factory and the construction of the unique stargate. The origin of a virus factory, in general only one per cell, and its development over time are also obscure. It has been reasonably suggested (17) that virus factories might be derived from the rough endoplasmic reticulum, which in amoebas is often localized at the margins of the nucleus (18–26). Indeed, there is persuasive evidence that this is the case for the virus factories of other large cytoplasmic viruses (17). A recent paper by Mutsafi et al. (27) describes the genesis of the membranes that compose the mimivirus factories, and those authors also concluded that the rough endoplasmic reticulum is the likely source.

Our primary objective in this investigation was to interrupt viral infection at sequential stages and visualize by AFM those structural intermediates present in infected cells. Care was taken to disrupt the cells as gently as possible so as to minimally perturb the structures, avoid dispersion, and, as best as possible, preserve the spatial relationships between structural features. From the observations, assembled in a temporal sequence, we attempted to reconstruct the assembly pathway. In most cases, this was less difficult than anticipated. Although the synchrony of infected cells was only marginal at best, thousands of AFM images, only some of which are presented here (see also the data posted at http://ucimcphersonlab.wikispaces.com/Mimivirus), provided ample and usually highly redundant observations. From these observations, we deduced what we believe is a convincing and relatively comprehensive morphogenetic pathway. This is not to say that the picture is completely clear. AFM is limited in what it can detect and record, as are all visualization methods at the nanoscale level. Thus, some structures and operations that exist within dense bodies or are otherwise obscured, such as the DNA-filling process, remained inaccessible.

Some specific questions addressed by this investigation, conducted using AFM applied to amoeba cells that were infected with mimivirus, and for which we provide at least partial answers are the origin and development of the virus factory, the morphogenesis of the capsid, the acquisition of the integument and surface fiber layers, and the overall assembly sequence of the virus. Combining our observations and deductions with those from previous works, both our own and those of others, we propose a pathway for assembly of the virus in amoebas.

MATERIALS AND METHODS

Virus propagation and infection, and sample preparation. *Acanthamoeba polyphaga* amoebas were grown in sterile Neff medium (ATCC 712 PYG) at 25°C to confluence in volumes of 25 ml, infected with mimivirus at ratios of about 10 to 1, and incubated at 25°C. Samples for AFM analysis were drawn at intervals p.i. as needed for the experiments. Cells could be preserved for fairly long periods of days to weeks by placing them at 4°C. Purified virus, however, was somewhat sensitive and deteriorated with time, even at 4°C.

Disruption of infected amoebas at periodic intervals in such a way that cell contents were not purged vigorously from the broken cells and spread over a large area of the AFM substrate was more challenging than we anticipated. Most recommended methods, such as osmotic shock or mild chemical treatments, did not break open the cells at all, or others, such as high-pressure release or sonication, essentially caused the cells to explode violently and scatter debris. Ultimately, we found that if the medium in which infected cells were grown was replaced with water, when the cells were dried on the AFM substrate, they would split open at the last moment. This provided optimal samples for imaging. In some cases, however, additional efforts were required. We found that replacement of culture media with distilled water and then freezing and thawing also gently disrupted infected cells. *In situ* disruption could be achieved by freezing and thawing samples thus treated directly on the AFM substrate. If freezing and thawing were carried out on infected cells in their culture media, disruption of cells seldom occurred, and neither approach consistently worked with uninfected cells. While some dispersion of cell contents was unavoidable, even with these processes, it was limited to an acceptable degree. Replacement of media was carried out by low-speed centrifugation to soft pellet the cells, removing the supernatant, and replacing it with water.

Following application of the infected cells to substrates, usually freshly cleaved mica coated lightly with poly-L-lysine, excess material was washed away, and the cells were disrupted as described above. The sample on the substrate was then exposed to 5% glutaraldehyde for 5 to 10 min, the excess was removed, the substrate was washed again with water, and the substrate with sample was dried in a stream of dry nitrogen gas at room temperature. Images were recorded primarily from dried samples, but some images were also collected in the culture media or in water to verify certain observations, to evaluate whether drying had created artifact, and to obtain some dimensions from fully hydrated material. Although AFM analysis (28, 29) was generally carried out in air, when scanning was performed in culture media or water, it was done in a fluid cell. Most technical details of the AFM analyses have been presented in previous papers (30–36).

AFM analysis. AFM imaging was carried out by using a Nanoscope III multimode instrument (Bruker Instruments, Santa Barbara, CA). When scanned in liquids, virus and associated macromolecules were scanned at 26°C by using oxide-sharpened silicon nitride tips in a 75-μl cell containing medium. For scanning in air, silicon tips were employed. The images were collected in the tapping mode (37, 38), with oscillation frequencies of

9.2 kHz in fluid and 300 kHz in air and with a scan frequency of 1 Hz. Vertical and lateral distances were calibrated by using standards from Digital Instruments (Santa Barbara, CA) with a step height of 10 nm and with a pitch of 200 nm and by using standards from MCNC Analytical Labs with a step height of 10 nm and a pitch of 1 μm. The AFM instrument was calibrated to small lateral distances by imaging the 111 face of a thaumatin protein crystal and using the known lattice spacings (39, 40) as the standard. Cantilevers for scanning in air were obtained from Bruker (Santa Barbara, CA) and were TAP150 with lengths of 115 to 135 μm and spring constants of 5 nN. For solution scanning, the cantilevers were OTR4 with lengths of 100 μm and spring constants of 0.08 nN.

In the AFM images presented here, height above substrate is indicated by an increasingly lighter color. Thus, points very close to the substrate are dark, and those well above the substrate are white. Because lateral dimensions are distorted due to an AFM image being the convolution of the cantilever tip shape with the surface features scanned (41), quantitative measures of size were based, whenever possible, either on heights above the substrate or on center-to-center distances on particle surfaces.

RESULTS

Sequencing of assembly events. In this paper, the description of results frequently deals with the appearance of structural features and their development in a temporally sequential manner. However, a description of a sequence of events does not necessarily mean that the AFM observations were made by continually or periodically observing events in real time on the same sample. Rather, a temporal sequence of events in the assembly pathway was constructed by recording static images from many samples taken from a culture at periodic intervals p.i. In a set of recorded images of one sample taken at a particular time, however, many assembly intermediates were simultaneously present. These intermediates represented virus particles at virtually all stages of development.

Virus entry. Shortly after the exposure of amoebas to virus, virions were observed to be attached to cell surfaces in the process of entering host cells (see the data posted at http://ucimcphersonlab.wikispaces.com/Mimivirus). After entrance, however, AFM was an inefficient tool for monitoring the encapsulation of the particles into endosomes, virus uncoating, or the release of the encapsidated nucleic acid into the cell. These are singular events, almost impossible to isolate and observe by AFM from among the cell contents. The only useful observation regarding entry was that in most infections, multiple virus particles could be seen attached to a cell. In no cases could a stargate assembly be observed on these particles. Presumably, the stargate was always turned toward the host's surface. This is consistent with the proposal (14) that the stargate may have a role in cell entry. There were no signs that the cell actively extruded membrane and deliberately enveloped the virus.

Appearance of transport vesicles. The earliest indications of virus activity appeared between 1 1/2 and 2 h p.i., although the cells were poorly synchronized. By 2 h p.i., most cells had formed small membranous sacs, which are here termed "transport vesicles" for reasons that are presented below. When dried upon the substrate, these vesicles had heights of about 200 nm to 250 nm (Fig. 2). The transport vesicles rapidly increased in number and accumulated in the cell over a period of 1 to 2 h. At 4 h postinfection, much of the cell was congested with the vesicles. In AFM images, the transport vesicles are similar in appearance to the membrane sacs that enclose the DNA of vaccinia virus (42). The transport vesicles exhibited a variety of smooth shapes with diameters varying from 0.5 μm to 2.5 μm. They had granular surfaces that have also been observed in AFM images of protein-coated cellular membranes (Fig. 2). The transport vesicles were distinctly different from mimivirus particles at any of the latter's several stages of development. The flood of transport vesicles preceded the appearance of a recognizable virus factory.

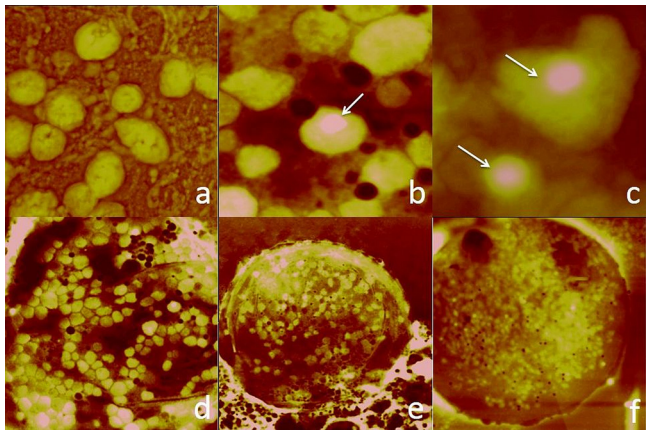

FIG 2 Transport vesicles are produced in great abundance at the borders of the nucleus at about 2 h postinfection (p.i.), and they ultimately flood the host cell cytoplasm by 3 to 4 h p.i. The transport vesicles appear smooth but irregular in shape, and they have dimensions ranging from about 1/2 μm to 2 1/2 μm. (a) The transport vesicles contain material that, when dispersed inside, gives them a uniform appearance. The internal material, however, frequently assumes a condensed state that manifests itself as a prominent bulge or protruding mass. (b and c) These bulges, some of which are marked by arrows, are seen most clearly as the intense white areas emerging from the vesicles. (d to f) AFM images of infected cells showing how the cytoplasm becomes increasingly congested with the transport vesicles. Coalescence of transport vesicles and initiation of virus factory formation are seen on the right in panel f. Scan areas are 5 μm by 5 μm (a and b), 2 μm by 2 μm (c), 30 μm by 30 μm (d), 40 μm by 40 μm (e), and 35 μm by 35 μm (f).

A quarter or more of the transport vesicles exhibited a single bud-like structure (Fig. 2b and c). The buds had a more or less uniform appearance with diameters that ranged from about 200 to 500 nm. The buds were relatively insensitive to AFM tip pressure, and they maintained their pronounced, distinctive shapes upon scanning. This suggested that they were not secondary, membranous vesicular buds originating from the surfaces of the transport vesicles. More likely, the protrusions or bulges are produced by the condensation of some material within the sacs. When the material is dispersed within the sacs, the transport vesicles are relatively flat and uniform in height, but when the material is condensed and vesicles are dried, bulges arising from the interior condensed masses become sensible to the AFM probe. Near their sites of origin, the transport vesicles were relatively flat and featureless, suggesting mostly dispersed material inside. As transport vesicles migrated further into the cytoplasm, protrusions became visible on more vesicles.

Origin of transport vesicles. The precise origin of the transport vesicles is not entirely clear. They were not present in uninfected cells, and they are not due to a rearrangement of preexisting vesicles or organelles. Presumably, they are the result of new synthesis following infection. Inspection of disrupted, infected cells, where the cell nucleus was intact and clearly defined, suggested that the transport vesicles were originating at the margins of the nucleus and conceivably budding from the nuclear membrane.

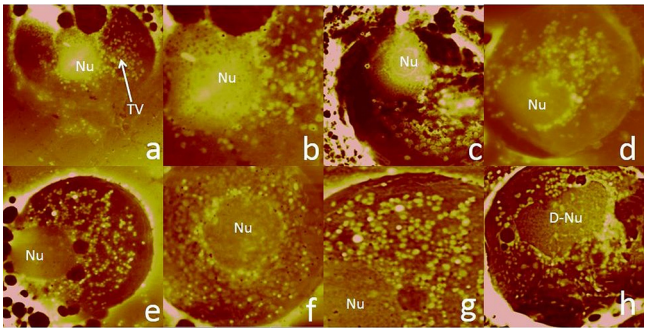

FIG 3 AFM images of an infected amoeba at about 2 h p.i. The prominent yolk-like bodies are cell nuclei (Nu). The image in panel b is a higher-magnification scan of the cell nucleus shown in panel a. Apparent in these images is that the transport vesicles (TV) originate at or near the borders of the nucleus, where they are densely clustered. They then stream outward from the nuclear borders to fill the cell. Many of the transport vesicles contain condensed material, while in others, it remains dispersed. A cell with a double nucleus (D-Nu) is shown in panel h. Scan areas are 30 μm by 30 μm (a), 15 μm by 15 μm (b), 30 μm by 30 μm (c), 30 μm by 30 μm (d), 20 μm by 20 μm (e), 20 μm by 20 μm (f), 20 μm by 20 μm (g), and 30 μm by 30 μm (h).

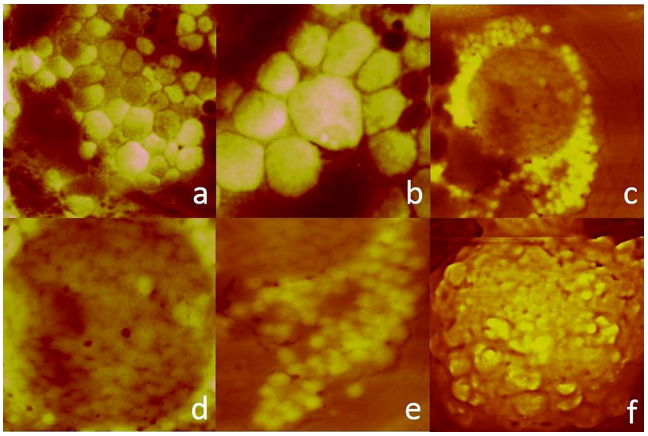

FIG 4 The transport vesicles begin coalescing once their density has reached some limit, and the clusters and larger aggregates take on the appearance of foam. Note the disparity of sizes and shapes of the transport vesicles within the clusters. The large mass seen in the AFM image in panel c contains many hundreds of transport vesicles that have condensed in preparation for virus factory formation. The interior of the central mass is seen at a higher magnification in panel d, and transport vesicles are shown at the bottom right edge in panel e. Note that as the aggregate evolves, many of the transport vesicles have rounded up and exhibit a late-stage globular form. An example where coalescence has advanced is shown in panel f. The transport vesicles have lost their structural individuality and have amalgamated. The body shown in panel f is a nascent virus factory. Scan areas are 10 μm by 10 μm (a), 5 μm by 5 μm (b), 20 μm by 20 μm (c), 10 μm by 10 μm (d and e), and 5 μm by 5 μm (f).

Indeed, AFM images, representative of many others (see the data posted at http://ucimcphersonlab.wikispaces.com/Mimivirus), clearly show emergence at the edges of the nucleus (Fig. 3). The generation of transport vesicles occurs at nuclear borders also in those cases of cells with double nuclei (Fig. 3h). The possibility of nuclear involvement therefore arises. If so, then the condensed material within transport vesicles could be inferred to be DNA. On the other hand, in amoebas and many other organisms, the rough endoplasmic reticulum is frequently localized near the nucleus of the cell and is very likely contiguous with the nuclear membrane (18–26). Therefore, it is equally possible, and perhaps more probable, that the transport vesicles do not have a nuclear membrane origin but are derived from the surrounding rough endoplasmic reticulum. As described below, transport vesicles are the precursors of virus factories, and virus factories must produce, in addition to nucleic acid, enormous quantities of proteins. It would therefore be advantageous if the vesicles transported, as at least part of their burden, ribosomes and the remaining protein synthetic apparatus that is indigenous to the rough endoplasmic reticulum.

Coalescence and condensation of transport vesicles. As the transport vesicles increase in number, they spread throughout the cytoplasm (Fig. 2d to f and 3). When their density reaches a certain level, they then begin to cluster and coalesce into foam (Fig. 4a and b). The possibility that the transport vesicles were mitochondria was considered, since these have roughly the same sizes and contain DNA, but these islands do not look similar to mitochondria when imaged by AFM, nor are they evident in uninfected cells.

In a recent paper (27) based on scanning-transmission electron microscopy tomography, Mutsafi et al. described membranous bodies in mimivirus-infected cells, at roughly the same time p.i., which they termed "cisternae" and whose properties are remarkably similar to the "transport vesicles" that we observed. The two are almost certainly the same. They concluded, as do we, that the cisternae play an important role in the development of mimivirus factories. They presented evidence that the "cisternae/transport vesicles" were the sources of virus factory membranes and furthermore also suggested, as we do, that they are likely derived from the rough endoplasmic reticulum.

At the same time, the protrusions and bulges on the transport vesicles that we believe are produced by condensed internal material suggest that they may contribute more than just membrane to the virus factories. Indeed, the transport vesicles may also be the same as the "strongly staining clusters" seen in EM images at roughly the same time p.i. (14). Those observations tend to support the hypothesis that the transport vesicles' cargo may include DNA, RNA, or both.

At 4 to 5 h p.i., masses of transport vesicles were present, both singly and in aggregates, and virus factories started to appear. Early stages of virus factory formation were often ambiguous, however, and it was frequently challenging to recognize them with certainty until they became productive and viral intermediates appeared on their surfaces. As virus factories developed, the number of transport vesicles decreased correspondingly, and there occurred a transition between the two. Transport vesicles continued to be generated, however, even when virus factories came into full production mode. Transport vesicles never disappeared completely, although they became sparse at later stages of infection.

Transport vesicles and formation of nascent virus factories. When cells were virtually filled with transport vesicles and their coalescence had advanced, more structurally organized aggregates of many hundreds of transport vesicles could be found, although there was generally no more than one, or a small number, per cell (Fig. 4c). An aggregate like that shown in Fig. 4c does not initially include all the transport vesicles in the cell, as many remain free and separate. As noted above, individual transport vesicles remain in the cell after virus factories have formed (Fig. 5). Ultimately, however, virtually all of the transport vesicles appear to be incorporated into aggregates (Fig. 4c) or into active virus factories

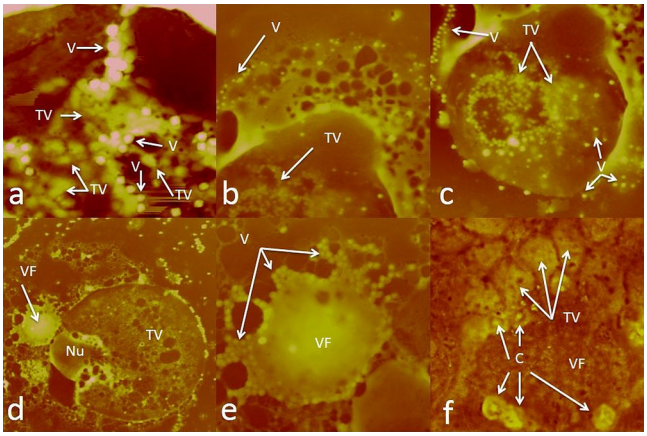

FIG 5 AFM images illustrating that even after virus factories have formed and are actively producing virus (V), transport vesicles (TV) continue to be generated and are presumably still joining productive virus factories (VF). Thus, virus factories and transport vesicles coexist in the same infected cell. In panel d, an active virus factory, seen at a higher magnification in panel e, has been ejected from an infected cell after disruption and lies immediately adjacent to a nucleus (Nu) at whose borders transport vesicles continue to appear. The bright spheres scattered in panels a to e are mature particles or capsids filled with DNA. At the end of the infection cycle, when cells burst as a consequence of virus accumulation, transport vesicles are scarcely present. Panel f shows a small area on the surface of a young virus factory. Seen simultaneously in this AFM image are a portion of the virus factory surface, transport vesicles merging into the virus factory, and assembling capsids (C) already emerging from the surface. Scan areas are 10 μm by 10 μm (a), 30 μm by 30 μm (b and c), 50 μm by 50 μm (d), 15 μm by 15 μm (e), and 5 μm by 5 μm (f).

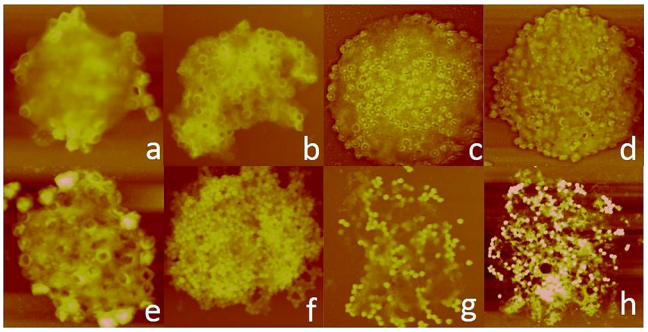

FIG 6 AFM images showing examples of virus factories arranged more or less according to their stages of development, ranging from rather young virus factories just beginning to produce capsids (a and b) to highly productive virus factories (c to f) and late-stage virus factories that are breaking up and dispersing throughout the cell (g and h). Note that in panel e, virions containing DNA, evidenced by their maintenance of shape, are present along with a large number of capsids that are either incomplete or complete but unfilled with DNA. The unfilled particles are recognizable by their collapse upon drying. Scan areas are 10 μm by 10 μm (a), 5 μm by 5 μm (b), 8 μm by 8 μm (c), 10 μm by 10 μm (d), 5 μm by 5 μm (e), 10 μm by 10 μm (f), 15 μm by 15 μm (g), and 25 μm by 25 μm (h).

(Fig. 5f). The transport vesicles tend to become rounder as they join the early aggregate (Fig. 4c and e) and begin to coalesce (Fig. 4f) and form nascent virus factories (Fig. 4c to f). A small area on the surface of an early virus factory (Fig. 4f) shows the simultaneous but distinct presence of both individual, merging transport vesicles and emerging capsids against the background of a virus factory surface.

Mutsafi et al. (27) reported that the cisterna progenitors of mimivirus factories, when in the proximity of factories, in turn generated buds that evolved into uniform 70-nm-diameter vesicles and that these secondary vesicles were integrated into the factories. We did not observe such secondary vesicles. However, they could have been lost from our samples in preparation or otherwise escaped detection by AFM. It was tempting to equate the buds that we observed on the transport vesicles with the 70-nm vesicles originating from their cisternae, but this seems problematic based on the discrepancy in physical size. The protrusions from the transport vesicles were 200 to 500 nm in diameter and not so uniform in size.

Viral factories. Viral factories, from which mimiviruses emerge, are essentially labyrinths of membranes responsible for the synthesis of the capsid components, the fabrication of icosahedral capsids, and their filling with nucleoprotein. The latter includes principally the genomic DNA and its associated proteins but probably some mRNA as well. A layer of integument protein is later added atop the capsid after release from the virus factory, and this serves to anchor the surface fibers to the virion. It is not entirely clear whether the process of integument protein addition, which appears to closely follow capsid assembly, is a function of the virus factory or is spatially distinct. The addition of the surface fibers occurs later and at a more distant locus that appears separated from the virus factory.

The proteins that comprise the outer layer of the virus factory must include the capsid coat proteins, or their precursors, and the proteins responsible for the genesis and assembly of the stargate. It seems unlikely that the viral proteins are synthesized in an interior aqueous region of the virus factory. This would require the proteins to subsequently be transported across a bilayer membrane to reach the surface. It further seems implausible that they, being membrane-associated proteins, are synthesized elsewhere in the cytoplasm of the cell and transported to the virus factory. It seems more probable that the capsid structural proteins are manufactured by ribosomes that are themselves embedded in or associated with the underlying membrane. Were this so, the proteins produced by the membrane-bound ribosomes could be extruded directly into or across the membrane, where they could accumulate on the surface of the virus factory. mRNA, necessary for protein synthesis, would be supplied to the ribosomes from the virus factory interior. This mechanism is consistent with the high level of protein synthesis that must occur in the production of protein capsids at the virus factory surface and with the hypothesis (17) that the membranes of the virus factories are derived from the rough endoplasmic reticulum.

Virus factories vary in size and appearance during the course of infection (Fig. 6; see also the data posted at http://ucimcphersonlab.wikispaces.com/Mimivirus). Initially, they are relatively small (5 to 10 μm in diameter) and dense and grow larger with time, and by the end of the infection cycle, when the cell is crowded with virus, the virus factories become highly disorganized and diffuse, filling virtually an entire cell. During their most productive phase, the virus factories are about 10 μm to 20 μm in diameter and are very soft, discrete, globular-shaped bodies. They are easily identified by the many viral intermediates emerging from their surfaces. When cells are gently disrupted, virus factories are frequently released from infected cells and can be seen isolated on the substrate. Thus, virus factories are not maintained firmly in place in the cell by cytoskeletal fibers or other

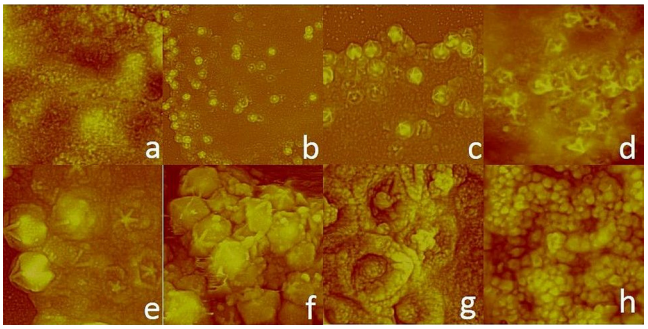

FIG 7 Variety of AFM images of areas on the surfaces of virus factories showing the range of activities and stages of development of virus particles. (a) Area where some capsids are about to begin forming but is otherwise free of incomplete particles. Apparent in this image is the rough, granular nature of the surface, which is essentially a continuous blanket of protein molecules resembling gravel at the nanoscale. The variegated pattern of light and dark (representing elevation) areas portends particle genesis. (b to h) Surface cluttered with virus capsids at all stages of development. These range from relatively sparse distributions of developing particles (b) to extremely dense accumulations of particles (h) that completely obscure the virus factory to which they remain attached. Panel g shows a higher-magnification image of several collapsed particles in fairly early stages of development, as indicated by their incomplete stargates, the lack of ordered surface lattice, and the absence of internal DNA. Note that in virtually all of the images, the vast majority of particles have collapsed and therefore have not yet been filled with DNA. This suggests that capsid formation is rapid, while filling with DNA lags substantially. Many of the particles in panel f, however, are still attached to the virus factory but have evidently been filled with DNA, as they have not collapsed. Scan areas are 1 μm by 1 μm (a), 10 μm by 10 μm (b), 5 μm by 5 μm (c), 3 μm by 3 μm (d), 2 μm by 2 μm (e), 2 μm by 2 μm (f), 1 μm by 1 μm (g), and 10 μm by 10 μm (h).

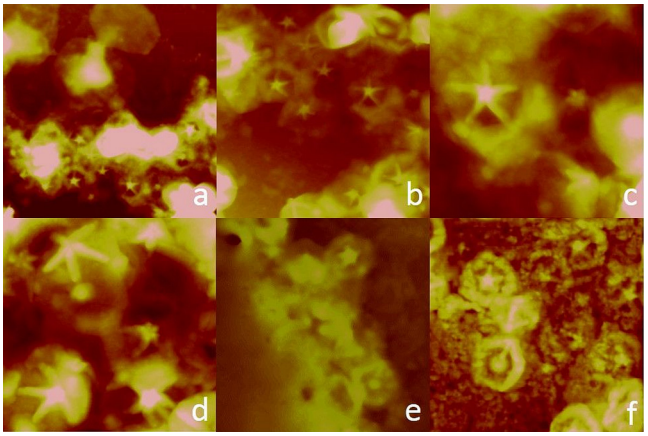

FIG 8 Mimivirus capsids are developed on spherical vesicles that bud out from the virus factory surfaces. The vesicles, which ultimately become both the icosahedral protein capsid and the internal membrane sac containing the viral DNA, consist, at minimum, of a lipid membrane thoroughly coated and likely embedded with structural and auxiliary proteins, including the coat protein or its precursors. The bubble-like vesicles are easily recognized because most are decorated with a stargate that appears at the initiation of capsid morphogenesis. At the contrast levels used to produce these images, the vesicles appear almost transparent, although they are virtually coated with proteins. In panel f, a high contrast level was applied, and this makes evident the rough, disordered protein surface of the vesicles that will subsequently compose itself into the fully formed icosahedral lattice. It is evident from these images that, initially, the proteins on the vesicle surfaces exhibit no geometrical order. Most of the vesicles shown in these images were still attached to fragments of dispersed virus factories. Scan areas are 3.5 μm by 3.5 μm (a), 2 μm by 2 μm (b), 1 μm by 1 μm (c), 1 μm by 1 μm (d), 3 μm by 3 μm (e), and 2 μm by 2 μm (f).

means of attachment. They are discrete bodies essentially independent of, or at best weakly bound by, the cellular matrix.

Virus factory surface activity. In our investigations, we benefitted from the response of capsid intermediates and completed particles to drying. When we recorded AFM images in air, upon drying, empty capsids or capsid intermediates collapsed, and deflated capsids appeared as double-walled, bowl-shaped objects. Capsids that had been filled with DNA, however, maintained their polyhedral shapes and proper dimensions. Thus, we could readily discriminate DNA-containing from unfilled capsids when scanning in air. In fluid, on the other hand, neither DNA-containing nor unfilled capsids collapsed. Figure 7 (see also the data posted at http://ucimcphersonlab.wikispaces.com/Mimivirus) presents a variety of AFM images, recorded on the productive surfaces of virus factories, showing the diverse nature of the events transpiring there, the range of morphological features, and the developing capsids. Virus factories imaged in air exhibited on their surfaces both DNA-filled particles leaving the virus factory surface as well as many otherwise complete but unfilled capsids. The latter were invariably in the majority and represented almost every stage in the morphogenesis of the capsids.

Vesicles serve as scaffolds for capsid morphogenesis. Mimivirus capsids are supported during their development by vesicles that emerge over time from the surface of a virus factory (Fig. 8); that is, as described in more detail below, the vesicles do not appear suddenly from the virus factory. In addition, they are true vesicles; that is, they are not produced by the budding of dense material or by particles passing through a membrane. The mimivirus vesicles, in terms of assembly, appear functionally homologous to the internal scaffolds that support the construction of icosahedral phage capsids (43–45).

Vesicle formation from biological membranes is a complicated and so far poorly understood process at the molecular level (46). In the case of mimivirus factories, a vesicle emerges from a surface composed of an underlying lipid bilayer membrane heavily coated with and/or embedded with a variety of proteins. Because the vesicles contain no dense material (prior to DNA entry), they are relatively soft, and when probed by AFM, they frequently appear almost transparent in images. Only when they have collapsed on a substrate and have been visualized at high contrast is their dense, granular surface apparent (Fig. 8).

The stargate and initiation of capsid assembly. The initial feature to appear in the morphogenesis of a viral capsid is an aggregate of proteins on the virus factory surface that becomes the center of the stargate. The stargate centers are not distributed according to any obvious pattern on the virus factory surface, appearing at seemingly arbitrary locations. The stargate center is a pentameric assembly of protein units that has a hole, or channel, along its unique axis that is maintained in the completed virion (Fig. 9). The pentamer serves as the nucleus for the development of the stargate. As the five arms of the stargate just begin forming, there is a thickening of the protein layer in its immediate vicinity, and with time, a rough disk of material, occasionally suggesting a polygonal form, accumulates around it (Fig. 9 and 10; see also the data posted at http://ucimcphersonlab.wikispaces.com/Mimivirus). The diameter of the disk is about that of a mature capsid. While the stargate nucleus initiates capsid formation, it seems that factors or events distant from the stargate determine or

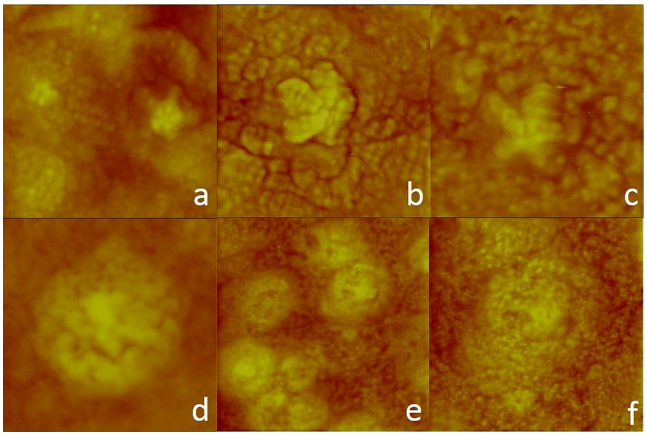

FIG 9 AFM images illustrating early stages of capsid morphogenesis. In virtually all cases, the first event is the appearance of a large pentameric protein assembly, presumably composed of five identical subunits, on the virus factory surface. In panels a to c, the appearance of the stargate center and the initiation of the five arms are shown. The arms do not necessarily all develop at the same rate, implying that their growth is not coordinated. A thickening of the protein layer in a disk shape is just perceptible, but in panel d, it is clearly evident. This provides the outline of an emergent vesicle. Note also that in panel d, only the center of the stargate is visible, but the disk of thickened protein is already prominent. The same is true of emerging vesicles/capsids in panels e and f, suggesting that only the central pentamers of the stargate may be necessary to signal capsid morphogenesis. Scan areas are 1 μm by 1 μm (a), 500 nm by 500 nm (b and c), 2 μm by 2 μm (d and e), and 1 μm by 1 μm (f).

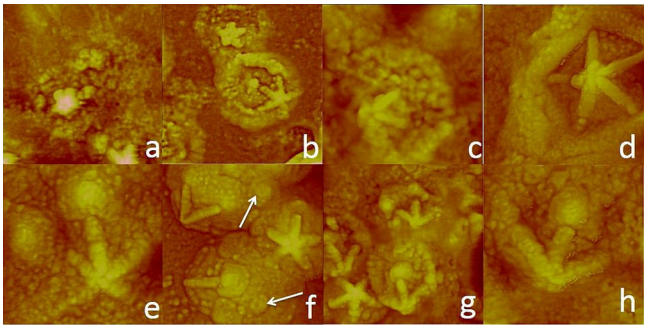

FIG 10 AFM images representing stages in the morphogenesis of the mimivirus capsid. (a to d) As events progress, the outer edge of the thickened disk takes on the appearance of a ridge. By the time the arms of the stargate have achieved almost full length, the disk has become an emerging vesicle/capsid. (e to h) Following or during completion of the stargate, prominent hillocks appear at locations occupied by 5-fold vertices in the completed icosahedral capsid. In panel f, the nuclei of some secondary, stargate-distal sets of 5-fold vertices are indicated by arrows. At the centers of the hillocks, pentameric proteins serve as nuclei for the development of an icosahedral lattice that eventually covers the surface. Scan areas are 1 μm by 1 μm (a and b), 500 nm by 500 nm (c to e), 1 μm by 1 μm (f and g), and 500 nm by 500 nm (h).

influence capsid architecture as well. The disk expands from the surface of the virus factory and forms a vesicle. Except for the stargate, the surface of the vesicle at this point displays no ordered arrangement, being simply a membrane vesicle whose surface is a confused, crowded, complex mass of proteins.

The stargate develops over time, probably over many minutes at least and perhaps longer. The arms do not necessarily elongate in a closely coordinated fashion. The arms of many stargates were of widely different lengths in some intermediate particles. When a stargate is complete, however, the arms are invariably all of the same length, and this length was always the same. The arms are composed of a basal layer consisting of two long sections that come together at a furrow along their parallel lengths. A second, somewhat narrower, superior layer lies over the central seam like a strip of "tape" (Fig. 1c). When the stargate opens to release DNA into a new host, the two sections of each arm split along their seam and fall away to allow five icosahedral faces to fold back. We conjecture that this splitting is probably promoted by the dissociation of the protein molecules making up the superior, tape layer of the arms. The basal layer of the stargate is in direct contact with the underlying membrane. It remains separate (although joined to) the coat protein lattice that later completes the icosahedral net.

Appearance of growth hillocks at pentameric vertices. When the stargate arms approach or reach their full extent, though in many cases where they are well short of terminal length, hillocks begin forming near the outer edges of the protein-cluttered disk/vesicle emerging from the virus factory surface (Fig. 10). The center points of these hillocks coincide exactly with the positions of the first ring of icosahedral 5-fold vertices nearest the stargate. Because terminal stargate arm length and hillock appearance are not necessarily sequential, it is unclear whether completed stargate arms determine the positions of the 5-fold vertices, whether the appearance of the 5-fold vertices determines the lengths of the stargate arms, or whether both are determined by some feature or property of the underlying membrane and are more or less independent of one another.

The peaks of the hillocks, the 5-fold vertices, are capped by pentameric oligomers of protein subunits (Fig. 11; see also the data posted at http://ucimcphersonlab.wikispaces.com/Mimivirus). These pentamers, by their considerably smaller size, are not the same as the pentameric protein oligomers that initiate the stargate. It is evident that the pentameric proteins are unique proteins and are not a consequence of any distortion or deformation of the coat protein hexameric lattice at the vertices. The pentamers serve as the unique nuclei for icosahedral lattice formation (Fig. 11). The hillocks at the vertices are steeper and more pronounced as the coat protein lattice spreads from their centers during morphogenesis than when the capsid is complete. The vertices do not protrude significantly on mature capsids (Fig. 1). This suggests that there may be some re-formation of capsid architecture or the underlying supporting membrane at some time, possibly when filling with DNA takes place.

The icosahedral coat protein lattice. As a vesicle emerges further from a virus factory surface, and lattice continues to spread over the vesicle surface from the five primary vertices, an additional ring of secondary 5-fold vertices begins to appear around the membrane-proximal end (stargate-distal end) of the particle. Each of these vertices in turn becomes a nucleus for icosahedral net formation (Fig. 11). Individual lattice islands, when their edges encounter one another, merge in a seamless manner to form the greater portion of the protein capsid (Fig. 12a). Figure 12b shows areas on incomplete particles that exhibit an icosahedral lattice but otherwise lack stargates. Figure 12c shows the emergence of 5-fold hillocks and the spread of the icosahedral net from their vertices, even in the absence of a stargate or its center. These images, though rare, imply that, at least under some circumstances, a stargate may not be essential to the appearance of 5-fold vertex hillocks or the subsequent production of the icosahedral lattice.

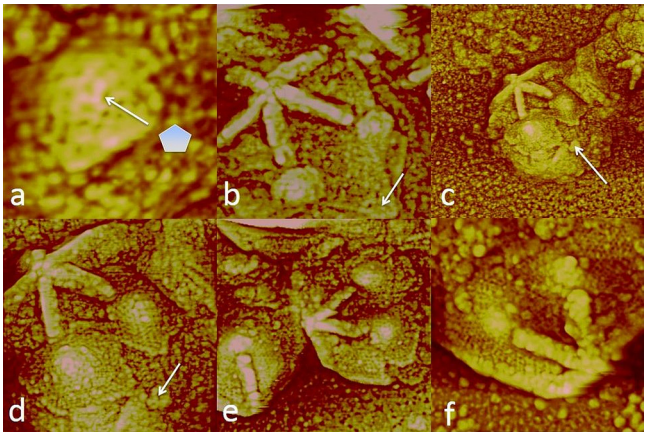

FIG 11 When the stargate arms have reached or are approaching their terminal lengths, hillocks capped by a pentameric protein at their peaks, marked by an arrow and a pentagon in panel a, appear spontaneously and precisely at the positions on the vesicle that will exhibit 5-fold vertices on the completed icosahedral capsid. This pentameric protein is not the same as that at the center of the stargate. It is significantly smaller and eventually integrates into the icosahedral capsid protein lattice without prominence. Beginning with this pentameric protein, which serves as a nucleus, the icosahedral lattice begins to appear, and this spreads outward from the hillocks in an approximately isometric manner. All 5-fold vertices do not appear simultaneously. Only the five nearest to the ends of the stargate arms first appear. After some development of the lattice from these vertices, the next set of five secondary vertices, some marked with arrows, emerges from the surface as similar hillocks. From all of the vertices, the respective lattice islands expand, encounter the edges of other lattice islands, and merge in a seamless manner to form the completed icosahedral capsid. As shown in panel f, lattice islands extend toward the stargate and fill in the gaps between the stargate arms, also joining to their edges without any visible discontinuity. Scan areas are 150 nm by 150 nm (a), 500 nm by 500 nm (b), 1 μm by 1 μm (c), 500 nm by 500 nm (d), 700 nm by 700 nm (e), and 500 nm by 500 nm (f).

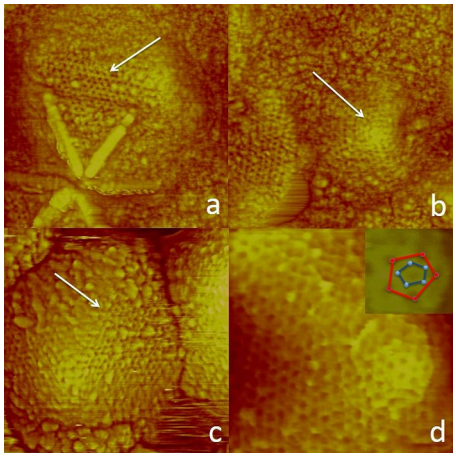

FIG 12 (a) The lattice islands from two vertices have merged (arrow) without any discontinuity, and the unified lattice front is now proceeding to fill the gap between two stargate arms. This has transpired while the vesicle/capsid has only partially emerged from the virus factory surface. (b) The surface of an emerging, apparently aberrant capsid, lacking any stargate at all, exhibits a large area covered by protein lattice (arrow), while the surface of the remainder of the particle is comprised of still disorganized protein. (c) An anomaly is presented. Fivefold vertices and the initial propagation of the icosahedral lattice (arrow) appeared on the virus factory surface in the absence of any stargate or thickened disk. The images in panels b and c suggest that the 5-fold vertices and icosahedral coat protein lattice can arise independently of a stargate and that their initiation is not necessarily dependent upon the development of a stargate. (d) AFM image of a developing 5-fold hillock made in fluid. The detail shows the pentagonal protein arrangement at the hillock center. Scanning in fluid yields a more realistic, undistorted image of the icosahedral protein lattice and emphasizes the three-dimensional nature of the thick honeycomb mesh. Scan areas are 500 nm by 500 nm for all images.

The membrane vesicle, on which a capsid is constructed, even as the capsid assembles and matures, remains contiguous with the underlying virus factory surface membrane. It is at this point that filling of the capsid with nucleic acid and its associated proteins occurs through the last remaining portal on the "backside" of a particle (3, 9, 14). Our observations suggest, however, that there is a significant temporal lag between capsid synthesis and filling with DNA or that the filling process is substantially slower, or perhaps less reliable, than capsid construction. We generally see a large number of unfilled but otherwise complete capsids surrounding virus factories and free in the cytoplasm compared with the number of filled particles at or near virus factory surfaces.

DNA and the filling process. AFM visualization of virus factory interiors was persistently obscured by the membrane/protein layer that covers the factory surface. The superior layer is furthermore relatively rigid and resistant to tip pressure when the glutaraldehyde-treated factories are dried. If, however, no fixation is carried out and the virus factories are simply dried on the substrate and then washed extensively, occasionally the surface layers are discarded. When that happens, images that show the distribution of DNA within are obtained (Fig. 13).

In Fig. 13, DNA is distributed throughout the interior of the factory and forms a vast reservoir of nucleic acid, presumably engaged in transcription and replication and also in preparation for filling of capsids. Some capsids still associated with the factory can be seen in Fig. 13. The presence of this mass of DNA in the interior of the factory is consistent with images obtained by others using electron microscopy (3, 9, 14). There is no obvious order or pattern to the arrangement of the nucleic acid as far as we can see, but this could be a consequence of the drying and washing of the sample, which render it collapsed upon a plane. It is possible that the apparent disorganization might be resolved if unperturbed in three dimensions. A feature worth noting is that the DNA, as shown in Fig. 13c, is highly condensed into thick cables and is associated with proteins. As described below, condensation and complexation with proteins are consistent with what is observed for DNA ejected from or encapsidated within virions.

We had initially assumed that once filling was complete, the

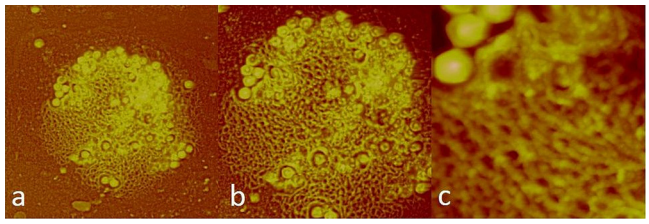

FIG 13 When the external membrane/protein layers of a virus factory are removed, the DNA matrix in the interior becomes exposed. (a and b) AFM images of the contents of an active virus factory showing the distribution of DNA (a) and the same sample scanned at a higher magnification (b). (c) High-magnification image of the nucleic acid showing the cables of condensed DNA heavily associated with proteins. The scan areas are 15 μm by 15 μm (a), 10 μm by 10 μm (b), and 3 μm by 3 μm (c).

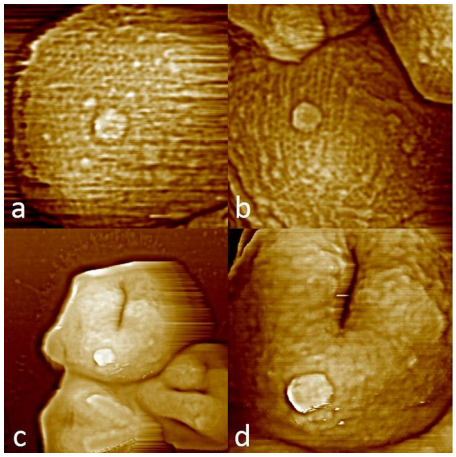

FIG 14 (a and b) Sides or facets of two independent capsids that are opposite the stargate and exhibit the 40-nm-diameter patch or plug that fills the DNA entry portal. No arms of the stargate are seen, confirming that the view is indeed of the side opposite the stargate. The icosahedral lattice is weakly visible in the neighborhood of the closure, validating the resolution of the images. (c and d) Another particle with a similar patch/plug seen at a lower magnification (c) and the closure at a higher magnification (d). Scan areas are 500 nm by 500 nm (a and b), 1 μm by 1 μm (c), and 500 nm by 500 nm (d).

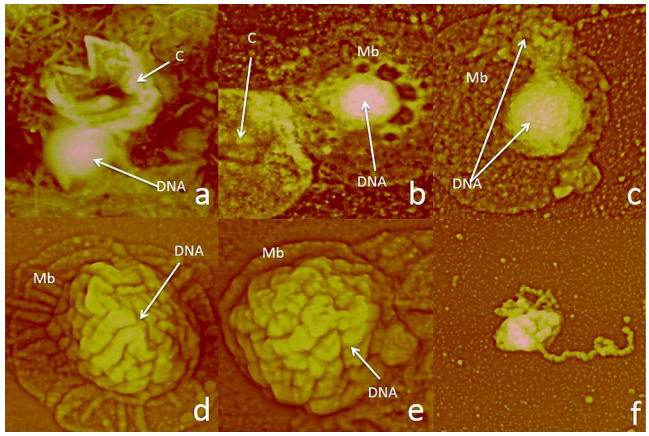

FIG 15 Mimivirus DNA (arrows) is present as highly condensed nucleoprotein masses about 350 nm in diameter within the inner membrane sacs (Mb) of virions. (a) Nucleoprotein-filled capsid that has spontaneously burst and ejected its almost spherical bolus of DNA. (b to d) Capsids that have expelled the internal membrane sacs containing their complements of DNA. The membranous sacs spread over the AFM substrate, leaving a bolus of DNA near their centers. In panel c, the DNA has begun to separate into strands. (e) DNA that is still compacted within a partial capsid, showing its highly convoluted, condensed form. (f) An isolated bolus of genomic DNA beginning to unravel, showing it to be composed of tightly wound, thick cables of the nucleic acid. Scan areas are 1.5 μm by 1.5 μm (a), 2 μm by 2 μm (b and c), 800 nm by 800 nm (d), 500 nm by 500 nm (e), and 3 μm by 3 μm (f).

portal on the backside of the capsid would be sealed by the continued formation of the icosahedral lattice so as to leave no "scar" or other evidence of its earlier presence. This appears not to be true, as we were able to record numerous images of capsids revealing their backside, where the portal is found. The portal is instead either patched or filled with a plug of protein (Fig. 14). We observed no icosahedral surface features on the closure, which is likely composed of another unique protein or, possibly, the capsid protein that is assembled in some alternate manner. The patch/plug, which protrudes from the capsid surface significantly, perhaps like the bung in a barrel, is consistently about 40 nm in diameter.

The portal for DNA entry was reported previously to be about 20 nm in diameter (3), about half the patch/plug diameter. The size discrepancy might be due in part to the different techniques employed, electron microscopy versus AFM, with the latter tending toward overestimates. On the other hand, if the plug has a conical shape, as do most rubber or cork stoppers, then it is not unreasonable that the observed diameter at the exterior exceeds the diameter of the hole which it fills. If the closure is instead a patch, then there is no size discrepancy.

We recorded numerous images of DNA that had been expelled from disrupted capsids or from their internal membrane sacs (Fig. 15). These images show that DNA, once inside a capsid, is highly condensed along with or because of associated proteins. The nucleoprotein fills the interior membrane sac. Much like vaccinia virus DNA (42), it is organized into thick trunks and cables that are then wrapped into tight, irregular bundles. There is no evidence to suggest any kind of spooling or regular folding of the nucleic acid within the capsids.

Acquisition of the integument protein layer. Following filling by nucleic acid or, in many cases, capsid formation without filling with DNA, mature capsids dissociate from the virus factory surface. Aside from capsids exhibiting an icosahedral net that are found near or at the surface of virus factories, however, naked capsids are rarely seen. It appears that shortly after completion and release from a virus factory, capsids acquire their integument protein layer. As shown in previous work (4) and further here as well, the integument protein is rather large and is likely an oligomer of smaller subunits, which would provide the multivalency required to anchor a number of surface fibers. The integument protein layer does not maintain the symmetry of the underlying capsid lattice.

The integument protein layer is acquired when a mature capsid, filled with DNA or not, passes through a membrane into which the integument protein is richly embedded. This is illustrated by the AFM images in Fig. 16. Indeed, inspection of most viral particles that are separated from a factory yet are still within a disrupted amoeba shows them to be capsids coated with the integument protein. Neither mature capsids exhibiting an icosahedral net nor particles coated with surface fibers are otherwise commonly seen. The integument protein-coated particles undoubtedly constitute the roughly 10% (3, 47) of the "bald" or "immature" particles that lack surface fibers.

We were not able to precisely localize the integument protein-bearing membrane. Although it does not appear to be an integral part of the virus factory, it must be very close by, perhaps concentric with the virus factory, like a penumbra. Indeed, in many AFM images of virus factories, including some presented here, the integument protein-containing membrane has collapsed over the factory surface and obscured its detailed features. In these images, both complete and incomplete particles, still attached to the factory surface, are shrouded in a layer of integument protein that prevents exposure of the capsids' icosahedral protein net.

The material character displayed by the integument protein-containing membrane is different from that of the virus factory membrane. It is more liquid and lacks the granularity of, for example, the transport vesicles (Fig. 16). Consistent with previous

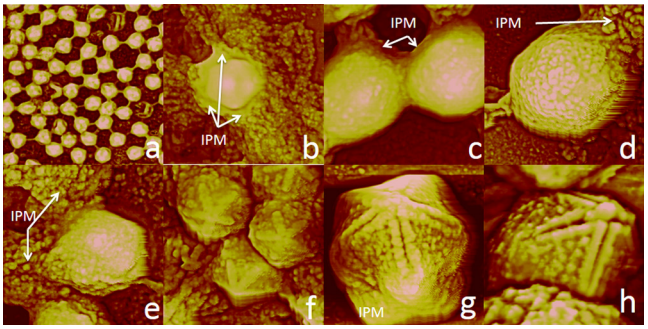

FIG 16 After the release of a capsid from the virus factory, filled or unfilled with DNA, it quickly passes through a lipid membrane thickly embedded with the integument protein responsible for anchoring the surface fibers. A mass of capsids is seen enmeshed in a membrane network (a), and individual particles or groups are seen passing through the membrane as they acquire a layer of membrane and integument protein (b to h). Arrows indicate trailing integument protein-laden membrane (IPM). The stargate, however, slips through the membrane without being thus coated. A capsid coated with integument protein presents a rather nondescript surface with no obvious geometrical order. In panels g and h, individual integument protein molecules can be seen on the particle surfaces. Note that the stargates of the particles in panels g and h have begun opening, revealing the longitudinal splitting of the stargate arms. Scan areas are 5 μm by 5 μm (a), 1.5 μm by 1.5 μm (b), 1 μm by 1 μm (c), 800 nm by 800 nm (d), 1 μm by 1 μm (e and f), 500 nm by 500 nm (g), and 550 nm by 550 nm (h).

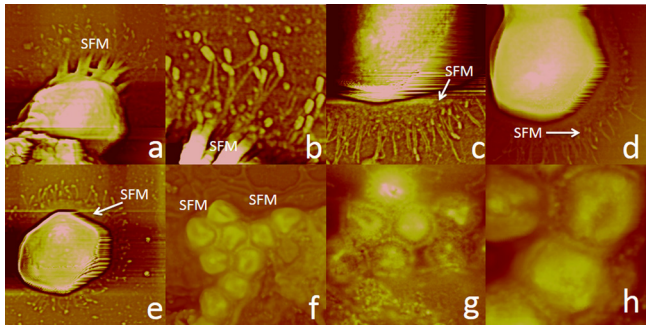

FIG 17 The last layer of structure to be added to a virion is the forest of surface fibers. The distal ends of the fibers are tipped by a globular protein head, with the opposite end fixed to the particle through an integument protein anchor. (a to e) Integument protein-coated particles encountering membranes, indicated by arrows and labeled SFM, whose outer surfaces are decorated with forests of surface fibers tipped with head groups. The surface fibers' tails are embedded in the lipid membrane. (f to h) Groups of virus that have acquired fibers by passing through the surface fiber-decorated membranes. Scan areas are 800 nm by 800 nm (a), 260 nm by 260 nm (b), 500 nm by 500 nm (c), 750 nm by 750 nm (d), 1 μm by 1 μm (e), 3.6 μm by 3.6 μm (f), 2.3 μm by 2.3 μm (g), and 1 μm by 1 μm (h).

observations (4), a layer of integument protein and its membrane coat the capsid generally but do not cover the stargate assembly. The stargate assembly ultimately remains free of surface fibers as a consequence. This implies that the proteins composing the stargate have a distinctly different character than the coat protein forming the capsid.

There was some question, arising in previous work (4), regarding whether the integument protein layer was composed of a unique protein or whether it was simply the extended polypeptide loops offered by the coat proteins forming the lattice (15). It is clear from the current results that the integument protein layer is indeed composed of a unique protein thoroughly embedded in a membrane matrix. Something, however, must effectively provide an adhesive to bind the integument protein to the coat protein layer. The large mobile loops of the underlying coat proteins seem to be the best candidates.

Acquisition of surface fibers. The final stage before lysis and release from the cell is the acquisition of surface fibers. This occurs only at a late stage and likely nearer the periphery of the cell. Only rarely were particles that bore surface fibers observed within the interior of cells, and they were never observed near virus factory surfaces. As noted above, most particles on the interior exhibit chiefly the integument layer to which the ends of surface fibers are ultimately attached.

Acquisition of surface fibers occurs in a manner similar to that by which the integument protein layer is added; that is, the integument protein-coated capsids pass further through membranes in a directional manner (Fig. 17). One side of the membrane, the entry side, is smooth, and the opposite side is forested with surface fibers. These surface fibers are already equipped with their globular protein heads. The fibers are anchored in the membrane. Thus, the acquisition of surface fibers involves layering of a membrane/protein sheet (the integument protein layer) with a second membrane/protein sheet (the surface fiber layer), a confection essentially made by double dipping. Membranes bearing surface fibers are visibly smoother and less cluttered with embedded proteins than are surfaces of transport vesicles, virus factories, or the membranes bearing the integument proteins. Hence, they too are likely derived from a different source and probably possess a significantly different composition and character.

The 7-nm periodic fibers. It remains uncertain whether surface fibers are made individually or whether they are "cut to length" from a longer fiber by proteolysis. The surface fiber protein must contain potential cleavage sites, however, as evidenced by their protection through glycosylation and the observation that they can be removed from the virion by the action of the protease bromelain (2, 4).

The close proximity of objects or features in an AFM image is not necessarily indicative of a structural relationship; it could simply be chance, but proximity in time and space is frequently meaningful. That is, objects in isolation and close to one another are at least suggestive of a relationship. Figure 18 provides an interesting and possibly significant example. The arrows in the low-magnification image in Fig. 18a indicate a long tangled fiber at the left and a small, indistinct object at the right. Higher-magnification AFM images in Fig. 18b and c show the tangled fiber in more detail and allow its identification as a long, 7-nm, periodic fiber, like that described in our previous AFM analyses (4). The small object in Fig. 18a is shown at a higher magnification in Fig. 18d to be a cluster of surface fibers attached to a fragment of the integument layer. We did not see examples of the two appearing separately. The simultaneous appearance of the long fiber and the surface fiber cluster in the same image is suggestive that the former may be a progenitor of the latter.

DISCUSSION

Transport vesicles and the origin and development of virus factories. The earliest event p.i. that can be ascribed to mimivirus activity and that is observable by AFM is the appearance of transport vesicles. These are seen at about 1 1/2 to 2 h p.i. By about 3 to 4 h p.i., the transport vesicles can, in some cases, almost fill the

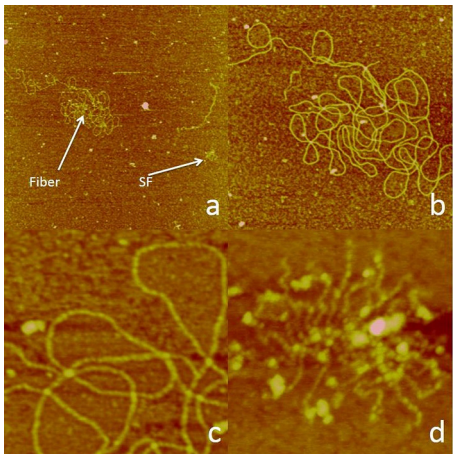

FIG 18 (a) The tangle of a long fiber (arrow) near a cluster of surface fibers (SF) (arrow). (b and c) The long fiber shown at a higher magnification. Panel c shows that the fiber exhibits a 7-nm periodicity along its length, as did fibers previously reported to be associated with mimivirus (4). (d) Higher-magnification image of the surface fiber cluster indicated by the arrow in panel a. Scan areas are 1 μm by 1 μm (a), 500 nm by 500 nm (b), 250 nm by 250 nm (c), and 300 nm by 300 nm (d).

cytoplasm of an infected amoeba cell. Virus factories may or may not already be identifiable at the end of this period. Transport vesicles originate at or very near the nuclear membrane, but because of their intimate association, transport vesicles could be derived from either the nuclear membrane or the rough endoplasmic reticulum. We favor the latter.

Fluorescence experiments show that the DNA from several large cytoplasmic viruses (17), including mimivirus (14), enters the nucleus and perhaps undergoes at least some rounds of replication. Other studies indicate that DNA replication is entirely cytoplasmic, with no nuclear entry (16). In the latter report, however, some "involvement of nuclear material" was considered possible. We see that at all stages of viral infection, there is no perceptible change in the shape, size, texture, or any other observable features of the nucleus. Even at the latest stages of infection, when the cell has burst and the virus factory is dispersed, the nucleus appears isolated and intact (Fig. 3 and 5). Our experiments do not resolve the question of DNA entry into the nucleus, but they do allow for this possibility. In any case, however, the morphology of the nucleus shows no evidence of change during infection.

Transport vesicles appear to contain some material, other than fluid, that is dispersed within most and condensed within others. When transport vesicles are dried upon the substrate, the condensed material is manifested as distinct bulges, buds, or protrusions from the otherwise leveled sacs. These are a consequence of the resistance of the interior condensed material to the pressure of the AFM cantilever tip. The surfaces of the sacs containing both condensed material and dispersed material appear the same. We believe that the transport vesicles serve as vessels to carry cargo from the nuclear region to virus factories, and we suggest that the material within the transport vesicles may be nucleic acid, possibly DNA, destined for delivery to a developing or active virus factory. The work of Mutsafi et al. (16) shows that the vesicles, which they termed cisternae, also provide a source of membranes for virus factory construction.

As virus factories enlarge, the amount of free transport vesicles decreases as transport vesicles continue to be absorbed by virus factories. Thus, it seems reasonable to conclude that the virus factories are derived, through the transport vesicles, from either the nuclear membrane, the contiguous rough endoplasmic reticulum, or both. Protein synthetic machinery, including ribosomes, may be synthesized in virus factories, but they are more likely also delivered by the transport vesicles. Even in cells with highly productive virus factories, as evidenced by the number of particles and their intermediates, transport vesicles are still relatively abundant in the cytoplasm to provide resupply. By the time of cell lysis, however, there are generally few remaining.

Structure and activities of virus factories. The template-dependent replication of DNA requires, of course, that an initial copy or copies initiate the process. The existence of a DNA mass in the virus factory interior says nothing, however, about the source of that initial DNA, whether it is present in some virus factory nucleus or core, about which a factory develops, or whether it is made elsewhere and delivered there, either initially or continuously, along with essential enzymes. Electron microscopy is more sensitive to the presence of electron-dense material such as DNA than is AFM, and EM has shown that the quantity of electron-dense material, presumably DNA, increases in virus factories in parallel with factory development (14). However, this does not necessarily imply that the increase is a consequence of DNA synthesized exclusively within the factory. DNA could well be replicated in the virus factory interior, but it could also be brought there from elsewhere by transport vesicles.

Given the quantity of capsids produced on a virus factory surface, it is obvious that a virus factory is responsible for massive amounts of protein synthesis for fabrication of protein capsids and their stargates as well as proteins that associate with nucleic acid and accompany DNA into the virion. There is no evidence to suggest that capsid proteins are synthesized elsewhere in the cell and transported through the cytoplasm to the virus factory surface. From our images, we estimate, for example, that somewhere between 1,000 and 2,000 particles may be made by a virus factory, from which it can be calculated that 1 million to 2 million copies of the coat protein alone must be made. The extent of protein synthesis required of the virus factory is a further argument that virus factories are derived from the rough endoplasmic reticulum. Only the rough endoplasmic reticulum could provide the necessary complement of active ribosomes for this amount of protein synthesis.

Structurally, a virus factory appears to be little more than an accordion-like mass of membranes, probably permeated with ribosomes and coated with a dense layer of membrane-associated protein. The virus factory entraps liquid containing the nucleic acid and the other necessary soluble enzymatic machinery for capsid and DNA synthesis. Virus factories, when scanned by AFM in fluid, have substantial three-dimensional forms; i.e., they are roughly globular, but virus factories dried on the substrate are rather flat, generally exhibiting heights above the substrate of little more than a micrometer. There is no indication of any rigid skeletal network reinforcing the internal space of the factories.

A perplexing but persistent observation was that some cells that were clearly producing virus particles appeared to lack an organized virus factory. Loss of factories from disrupted cells is an inadequate explanation given the number of examples and their circumstances. It must be considered that some virus may be pro-

duced from clusters of transport vesicles so small that they are unrecognizable as conventional virus factories. Thus, the lower limit on virus factory size may be significantly less than that suggested by the images shown in Fig. 6. On the other hand, no stargate was ever observed on an individual transport vesicle. Thus, we conclude that whatever is borne by such a vesicle, it is alone insufficient to give rise to a virus capsid.

As might have been anticipated from previous electron microscopy studies, the DNA in mature virus factories was seen to compose a vast reservoir in the interior. The DNA displayed no apparent organization and was more or less uniformly distributed. It was highly condensed and heavily associated with proteins. Our study sheds no additional light on the filling process itself, although the notable lag between capsid morphogenesis and filling suggests that the latter may be the rate-limiting step in virion construction.

Morphogenesis of the capsid. A capsid assembly pathway consistent with AFM images is illustrated in Fig. 19a. On the surface of the virus factory membrane, crowded with a dense and disordered layer of proteins, the pentameric center of a stargate appears. The time and place of this initial event are, as far as we can tell, arbitrary. This is followed, not necessarily sequentially or in a closely coordinated manner, by (i) the growth from the pentamer of the arms of the stargate, (ii) the thickening of a disk with roughly the diameter of a full capsid, (iii) the formation of a raised ridge around the circumference of the disk that occasionally exhibits intimations of a pentagonal figure, (iv) the appearance of 5-fold vertices nearest to the stargate arm termini of the future icosahedron, (v) the nucleation and spread of the icosahedral protein lattice outward from those vertex pentamers, (vi) the appearance of stargate-distal vertices and the spread of lattice from these vertices, (vii) the semicompletion of the capsid net as lattice islands merge (one face remains open and contiguous with the interior of the virus factory to allow DNA filling) and completion of the stargate, (viii) the filling of the capsid with DNA and other associated macromolecules (not observable by AFM), (ix) the sealing of the DNA entry portal by a protein plug, and (x) the release of the filled virion (as well as some unfilled virions) from the surface of the virus factory. While the 5th to 10th events are always sequential, the earliest events (1st to 4th) do not consistently appear to be so, although they do generally follow one another in that order.

Because of the absence of a consistent correlation between stargate arm completion and pentameric vertex emergence, the apparent absence of direct physical continuity between them, the lack of obvious cause (stargate arm completion) and effect (5-fold vertex appearance), and the observed anomalies (Fig. 12b and c) where no stargate was present, we have come to believe that the stargate does not directly, or possibly even indirectly, specify the location of the 5-fold vertices. Furthermore, while this might still be plausible for the first set of 5-fold vertices at the "ends" of the stargate arms, it is difficult physically to see how the next ring (stargate distal) of secondary 5-fold vertices on the icosahedron could also be specified by the stargate. Finally, the precision with which the locations of the 5-fold vertices are specified is extraordinary. Two salient questions emerge. What determines the lengths of the stargate arms, and what specifies the precise locations of the 5-fold vertices? If mechanisms could be found that provide answers to these two questions, issues having homologues common in embryogenesis and development, then in a conceptual sense, the remainder of capsid morphogenesis is explicable in terms of our present understanding of macromolecular structure and how macromolecules interact among themselves.

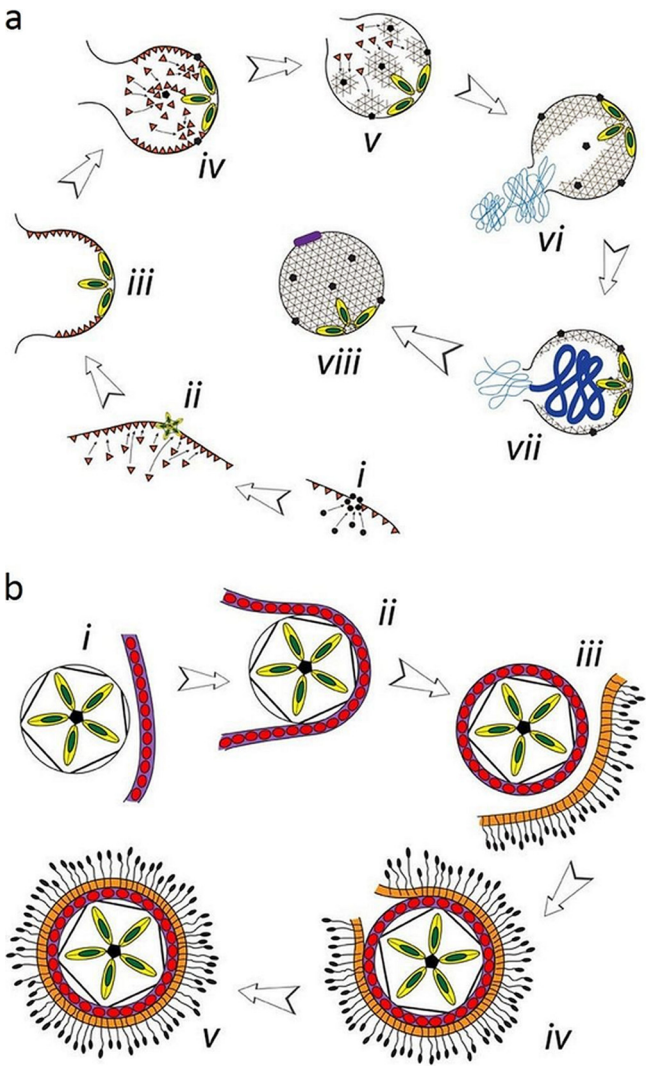

FIG 19 Schematic diagrams summarizing the steps most generally observed in capsid formation up to its release from a virus factory (a) and outlining the final steps in mimivirus morphogenesis, the acquisition of an integument layer and coating of surface fibers (b). (a) Capsid morphogenesis begins on the virus factory surface (i) by the formation of a stargate central pentamer (ii), initial growth of stargate arms, thickening of a capsid disk, and initial emergence of a vesicle, shown more fully developed (iii). Pentamer-capped hillocks appear at eventual 5-fold vertices (iv), and these hillocks serve as nuclei for the development of the coat protein, icosahedral net (v). Upon completion of the protein capsid (vi), the DNA is poised to enter the empty capsid through a stargate-distal portal, which it does (vii) as the nucleic acid condenses inside. The entry portal is sealed (viii) to yield a completed capsid. (b) The superior structural layers are acquired when a capsid (i) passes sequentially through a membrane embedded with integument protein (ii) and then through a membrane containing on its distal side a coating of surface fibers (iii and iv). This results in the completed virion (v).

Acquisition of the integument protein and surface fiber layers. Our AFM investigation demonstrates that both the integument protein layer of a virion and the layer of surface fibers are acquired by the capsid passing through two membranes in succession (Fig. 19b). The membrane containing the integument protein is near the virus factory surface, possibly closely concentric with it,

as very few naked capsids were ever observed in a cell except at or near a factory. Most cytoplasmic particles were seen to be coated with integument protein but to lack surface fibers. Conversely, particles at the periphery of the cell generally had acquired surface fibers. The latter suggests that the membranes providing the surface fibers are located at some distance from a factory.

The source of surface fibers continues to be a puzzle. It seems unlikely that the fibers, which consist of a stalk with an attached protein head, are synthesized individually on a membrane and then modified by glycosylation. The surface fibers do not all have exactly the same length and are therefore not all identical. Second, it would seem inefficient to make and treat each surface fiber individually. We favor, but cannot verify, that a mechanism probably exists by which long fibers are synthesized, modified, and then clipped into appropriate lengths by proteases.

Certain observations support this hypothesis. In previous papers (4, 48), we described ordered assemblies of fibers having 7-nm linear periodicity. We were unable to identify definitively the origin or the purpose of the fibers, although we suggested that by cleavage, they might provide the shafts of surface fibers. Their dimensions and general features were consistent with this hypothesis. We have again observed the presence of these fibers in infected amoebas (Fig. 18), consistent with a role in virus development. How the fibers, after scission, become embedded in a membrane and how the protein heads become attached remain unknown.

Recently, an electron micrograph from the group of Raoult (see Fig. 2B in reference 49) came to our attention, which further supported this hypothesis. In that micrograph of a negatively stained mimivirus, the shafts of many of the surface fibers showed distinctive, periodic patterns of light and dark. The period of the pattern, using the micrograph distance standard, was 7 nm, exactly the same period exhibited by the long fibers that we previously described and have visualized again in this investigation.

An assembly pathway for mimivirus. The AFM image data combined with previous data available from AFM, X-ray diffraction, fluorescence, and several EM studies support the schematic models in Fig. 19a and b as a plausible morphogenetic pathway for mimivirus. Figure 19a illustrates the steps leading to capsid formation and the filling of the capsid with nucleic acid, followed, as shown in Fig. 19b, by the acquisition of the integument protein layer and the covering of surface fibers. The model will have to evolve with time and the appearance of new data, but at this point, we believe that it reconciles most of the observations and presents a relatively comprehensive hypothesis.

REFERENCES

1. **Xiao C, Chipman PR, Battisti AJ, Bowman VD, Renesto P, Raoult D, Rossmann MG.** 2005. Cryo-electron microscopy of the giant Mimivirus. J. Mol. Biol. **353:**493–496.
2. **Xiao C, Kuznetsov YG, Sun S, Hafenstein SL, Kostyuchenko VA, Chipman PR, Suzan-Monti M, Raoult D, McPherson A, Rossmann MG.** 2009. Structural studies of the giant mimivirus. PLoS Biol. **7:**e92. doi:10.1371/journal.pbio.1000092.
3. **Zauberman N, Mutsafi Y, Halevy DB, Shimoni E, Klein E, Xiao C, Sun S, Minsky A.** 2008. Distinct DNA exit and packaging portals in the virus Acanthamoeba polyphaga mimivirus. PLoS Biol. **6:**e114. doi:10.1371/journal.pbio.0060114.
4. **Kuznetsov YG, Xiao C, Sun S, Raoult D, Rossmann M, McPherson A.** 2010. Atomic force microscopy investigation of the giant mimivirus. Virology **404:**127–137.
5. **Raoult D, Audic S, Robert C, Abergel C, Renesto P, Ogata H, La Scola B, Suzan M, Claverie JM.** 2004. The 1.2-megabase genome sequence of Mimivirus. Science **306:**1344–1350.
6. **Benson SD, Bamford JK, Bamford DH, Burnett RM.** 2004. Does common architecture reveal a viral lineage spanning all three domains of life? Mol. Cell **16:**673–685.
7. **Claverie JM, Ogata H, Audic S, Abergel C, Suhre K, Fournier PE.** 2006. Mimivirus and the emerging concept of "giant" virus. Virus Res. **117:**133–144.
8. **Raoult D, Forterre P.** 2008. Redefining viruses: lessons from Mimivirus. Nat. Rev. Microbiol. **6:**315–319.
9. **Suzan-Monti M, La Scola B, Raoult D.** 2006. Genomic and evolutionary aspects of Mimivirus. Virus Res. **117:**145–155.
10. **Claverie JM, Grzela R, Lartigue A, Bernadac A, Nitsche S, Vacelet J, Ogata H, Abergel C.** 2009. Mimivirus & Mimiviridae: giant viruses with an increasing number of potential hosts, including corals and sponges. J. Invertebr. Pathol. **101:**172–180.
11. **Iyer LM, Aravind L, Koonin EV.** 2001. Common origin of four diverse families of large eukaryotic DNA viruses. J. Virol. **75:**11720–11734.
12. **Van Etten JL, Lane LC, Meints RH.** 1991. Viruses and viruslike particles of eukaryotic algae. Microbiol. Rev. **55:**586–620.
13. **Yamada T, Onimatsu H, Van Etten JL.** 2006. Chlorella viruses. Adv. Virus Res. **66:**293–336.
14. **Suzan-Monti M, La Scola B, Barrassi L, Espinosa L, Raoult D.** 2007. Ultrastructural characterization of the giant volcano-like virus factory of Acanthamoeba polyphaga mimivirus. PLoS One **2:**e328. doi:10.1371/journal.pone.0000328.
15. **Klose T, Kuznetsov YG, Xiao C, Sun S, McPherson A, Rossmann MG.** 2010. The three-dimensional structure of Mimivirus. Intervirology **53:**268–273.
16. **Mutsafi Y, Zauberman N, Sabanay I, Minsky A.** 2010. Vaccinia-like cytoplasmic replication of the giant Mimivirus. Proc. Natl. Acad. Sci. U. S. A. **107:**5978–5982.
17. **Novoa RR, Calderita G, Arranz R, Fontana J, Granzow H, Risco C.** 2005. Virus factories: associations of cell organelles for viral replication and morphogenesis. Biol. Cell **97:**147–172.
18. **Anderson DJ, Hetzer MW.** 2008. Shaping the endoplasmic reticulum into the nuclear envelope. J. Cell Sci. **121:**137–142.
19. **Evans DE, Bryant JA, Hutchison C.** 2004. The nuclear envelope: a comparative overview. Symp. Soc. Exp. Biol. **2004:**1–8.
20. **Flickinger CJ.** 1969. The development of Golgi complexes and their dependence upon the nucleus inmebae. J. Cell Biol. **43:**250–262.
21. **Flickinger CJ.** 1977. Relationships between membranous organelles in amoebae studied by electron microscopic cytochemical staining. Cell Tissue Res. **180:**139–154.
22. **Flickinger CJ.** 1974. The role of endoplasmic reticulum in the repair of amoeba nuclear envelopes damaged microsurgically. J. Cell Sci. **14:**421–437.
23. **Lu L, Ladinsky MS, Kirchhausen T.** 2011. Formation of the postmitotic nuclear envelope from extended ER cisternae precedes nuclear pore assembly. J. Cell Biol. **194:**425–440.
24. **Mattaj IW.** 2004. Sorting out the nuclear envelope from the endoplasmic reticulum. Nat. Rev. Mol. Cell Biol. **5:**65–69.
25. **Mercer EH.** 1959. An electron microscopic study of Amoeba proteus. Proc. R Soc. Lond. B Biol. Sci. **150:**216–232.
26. **Shibata Y, Voeltz GK, Rapoport TA.** 2006. Rough sheets and smooth tubules. Cell **126:**435–439.
27. **Mutsafi Y, Shimoni E, Shimon A, Minsky A.** 2013. Membrane assembly during the infection cycle of the giant mimivirus. PLoS Pathog. **9:**e1003367. doi:10.1371/journal.ppat.1003367.
28. **Binnig G, Quate CF.** 1986. Atomic force microscope. Phys. Rev. Lett. **56:**930–933.
29. **Bustamante C, Keller D.** 1995. Scanning force microscopy in biology. Phys. Today **48:**32–38.
30. **Kuznetsov YG, Datta S, Kothari NH, Greenwood A, Fan H, McPherson A.** 2002. Atomic force microscopy investigation of fibroblasts infected with wild-type and mutant murine leukemia virus (MuLV). Biophys. J. **83:**3665–3674.
31. **Kuznetsov YG, Low A, Fan H, McPherson A.** 2005. Atomic force microscopy investigation of isolated virions of murine leukemia virus. J. Virol. **79:**1970–1974.
32. **Kuznetsov YG, Malkin AJ, Lucas RW, Plomp M, McPherson A.** 2001. Imaging of viruses by atomic force microscopy. J. Gen. Virol. **82:**2025–2034.

33. **Kuznetsov YG, McPherson A.** 2006. Atomic force microscopy investigation of Turnip yellow mosaic virus capsid disruption and RNA extrusion. Virology **352:**329–337.
34. **Kuznetsov YG, McPherson A.** 2006. Identification of DNA and RNA from retroviruses using ribonuclease A. Scanning **28:**278–281.
35. **Kuznetsov YG, Victoria J, Low GA, Robinson WE, Jr, Fan H, McPherson A.** 2004. Atomic force microscopy imaging of retroviruses: human immunodeficiency virus and murine leukemia virus. Scanning **26:**209–216.
36. **Malkin AJ, Plomp M, McPherson A.** 2004. Unraveling the architecture of viruses by high-resolution atomic force microscopy, p 85–108. *In* Lieberman PM (ed), Virus structure and imaging, DNA viruses, methods and protocols. Humana Press, Totowa, NJ.
37. **Hansma HG, Hoh JH.** 1994. Biomolecular imaging with the atomic force microscope. Annu. Rev. Biophys. Biomol. Struct. **23:**115–139.
38. **Hansma HG, Pietrasanta L.** 1998. Atomic force microscopy and other scanning probe microscopies. Curr. Opin. Chem. Biol. **2:**579–584.
39. **Ko TP, Day J, Greenwood A, McPherson A.** 1994. Structures of three crystal forms of the sweet protein thaumatin. Acta Crystallogr. D Biol. Crystallogr. **50:**813–825.
40. **Kuznetsov YG, Konnert J, Malkin AJ, McPherson A.** 1999. The advancement and structure of growth steps on thaumatin crystals visualized by atomic force microscopy at molecular resolution. Surf. Sci. **440:**69–80.
41. **Kuznetsov YG, McPherson A.** 2011. Atomic force microscopy in imaging of viruses and virus-infected cells. Microbiol. Mol. Biol. Rev. **75:**268–285.
42. **Kuznetsov Y, Gershon PD, McPherson A.** 2008. Atomic force microscopy investigation of vaccinia virus structure. J. Virol. **85:**7551–7566.
43. **Casjens S (ed).** 1997. Principles of virion structure, function, and assembly. Oxford University Press, Oxford, United Kingdom.
44. **King J.** 1971. Bacteriophage T4 tail assembly: four steps in core formation. J. Mol. Biol. **58:**693–709.
45. **Showe MK, Black LW.** 1973. Assembly core of bacteriophage T4: an intermediate in head formation. Nat. New Biol. **242:**70–75.
46. **Schmidt AA.** 2002. Membrane transport: the making of a vesicle. Nature **419:**347–349.
47. **Boyer M, Azza S, Barrassi L, Klose T, Compocasso A, Pagnier I, Fournous G, Borg A, Robert C, Zhang X, Desnues C, Henrissat B, Rossmann M, La Scola B, Raoult D.** 2011. Mimivirus shows dramatic genome reduction after intraamoebal culture. Proc. Natl. Acad. Sci. U. S. A. **108:**10296–10301.
48. **Kuznetsov YG, McPherson A.** 2010. Nano-fibers produced by viral infection of amoeba visualized by atomic force microscopy. Biopolymers **95:**234–239.
49. **Raoult D, La Scola B, Birtles R.** 2007. The discovery and characterization of Mimivirus, the largest known virus and putative pneumonia agent. Clin. Infect. Dis. **45:**95–102.